

Article

# The Influence of Different Facings of Polyisocyanurate Boards on Heat Transfer through the Wall Corners of Insulated Buildings

Tomas Makaveckas \* , Raimondas Bliudžius and Arūnas Burlingis

Building Physics Laboratory, Institute of Architecture and Construction, Kaunas University of Technology, Tunelio str. 60, 44405 Kaunas, Lithuania; raimondas.bliudzius@ktu.lt (R.B.); arunas.burlingis@ktu.lt (A.B.)

\* Correspondence: tomas.makaveckas@ktu.edu

Received: 27 March 2020; Accepted: 17 April 2020; Published: 17 April 2020



**Abstract:** Polyisocyanurate (PIR) thermal insulation boards faced with carboard, plastic, aluminum, or multilayer facings are used for thermal insulation of buildings. Facing materials are selected according to the conditions of use of PIR products. At the corners of the building where these products are joined, facings can be in the direction of the heat flux movement and significantly increase heat transfer through the linear thermal bridge formed in the connection of PIR boards with facing of both walls. Analyzing the installation of PIR thermal insulation products on the walls of a building, the structural schemes of linear thermal bridges were created, numerical calculations of the heat transfer coefficients of the linear thermal bridges were performed, and the influence of various facings on the heat transfer through the thermal bridge was evaluated. Furthermore, an experimental measurement using a heat flow meter apparatus was performed in order to confirm the results obtained by numerical calculation. This study provides more understanding concerning the necessity to evaluate the impact of different thermal conductivity facings on the heat transfer through corners of buildings insulated with PIR boards.

**Keywords:** heat transfer; polyisocyanurate boards; facings; thermal bridges; heat flux

## 1. Introduction

In the past few decades, tremendous development in the improvement of the energy efficiency of buildings has occurred and caused lower consumption of conventional fuel and CO<sub>2</sub> emissions that generate the greenhouse effect [1,2]. The building sector accounted for nearly 40% of the total energy consumption in the world [3,4] and was therefore responsible for quite high pollutant emissions. For this scope, the use of efficient insulating materials is often the key element reducing the heat losses through the building enclosures [5].

One of the most efficient thermal insulation materials, before widely used in different fields of industry and now increasingly applicable in the construction sector, is rigid polyisocyanurate-polyurethane foam (PIR/PUR) [6]. The use of PIR/PUR in the construction sector has increased due to its excellent mechanical properties and low thermal conductivity [7]. PIR insulation is the most widely used thermal insulation material in low-slope roofs in the U.S. (50–70% of the market share) [8]. This material is also widely used in the thermal insulation of walls [9]. For example, foil-faced PIR is used most as wall sheathing in residential construction or in masonry cavity wall construction [10], and it creates one of the greatest thermal resistance values (R-value) compared with other thermal insulation materials [11].

The largest volume of rigid PIR boards is produced in sheet form on machines known as laminators that are essentially double conveyors, between which foam rises to a controlled thickness. The faced

sheet products obtained on laminators are widely used for construction applications such as roofing or insulated facades [12].

The flexible facings are generally made of mineral fleece, glass fleece, aluminum foil, or composite film [13]. Depending on the type of facings of the PIR board, flexible-faced or rigid-faced PIR foam boards could be distinguished [12]. The choice of facing usually depends on the wall construction where the PIR thermal insulation will be installed. For example, PIR faced with thin aluminum foil is commonly used as exterior or interior continuous thermal insulation for masonry or concrete wall systems and in residential and commercial wood framework construction. PIR with plastic facing is usually used in the production of precast insulated concrete sandwich panels and in the construction of cast-in-place insulated concrete walls. The same applications exist for PIR faced with composite paper foil. Different types of facings are shown in Figure 1.

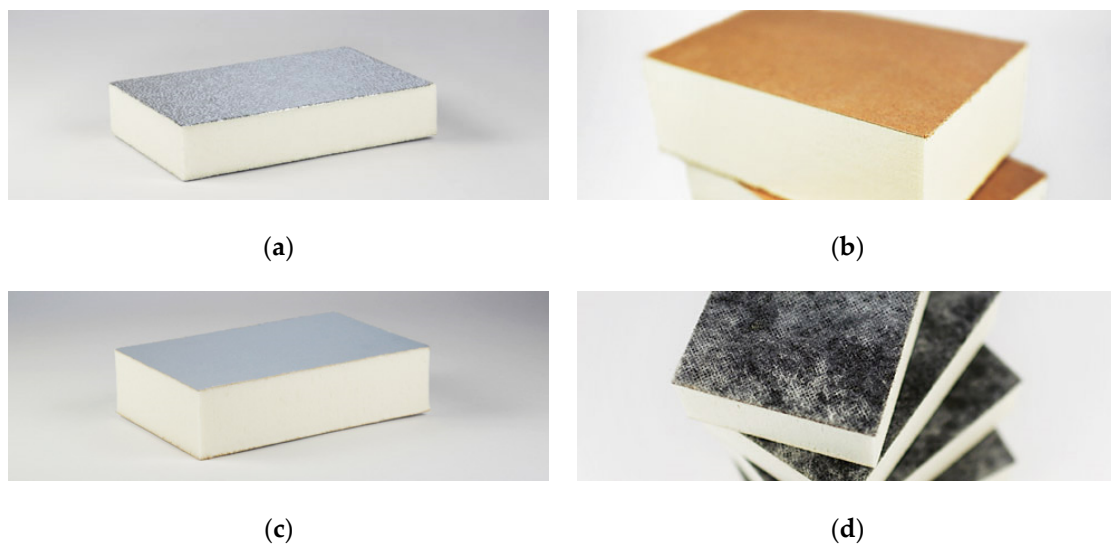


**Figure 1.** Types of polyisocyanurate (PIR) facings: (a) aluminum foil; (b) composite paper foil; (c) multilayer aluminized facing; (d) bitumen facing [14].

Different facings are chosen to match the intended application of the PIR insulation boards. The facings protect the foam core from the ultraviolet radiation (UV) degradation [10]. Facing materials serve a variety of functions in the production and use of PIR insulation. They are used to contain the foam core during the production process, creating the stability of the finished insulation board. Facings also may serve several functions during the exploitation phase of the product, in particular the contribution to strength and dimensional stability [15]. Different facings can create a vapor barrier, moisture lock, reflecting surface, or protection against mechanical damage [13].

Foil and plastic facings on rigid PIR foam panels are used to stabilize the R-value of the product, slowing down thermal conductivity drift and maintaining the long-term thermal resistance of the insulation [16]. When PIR is manufactured, many small closed cells are created. This means that the blowing agent vaporized during the foaming reaction fills these small cells [17]. To reach gas equilibrium, the air strives to migrate into the cells, and the blowing agent migrates out of the cells [16,18]. As a result, the composition of the gas in the cells changes, and the thermal conductivity of the PIR thermal insulation product increases over time [19]. Therefore, in order to maintain the initial thermal properties of polyisocyanurate foam, the aim is to minimize the damage to these facings during the installation of building insulation.

However, at the corners of the building where these products are joined together, facings can be positioned in the direction of the heat flux movement and might increase heat transfer through the linear thermal bridge formed in the corner of the building. Thermal bridges are parts of the

building envelope where the otherwise uniform thermal transfer is significantly changed, resulting in a multidimensional heat flow [20].

Much research was carried out to investigate the reduction in heat transmittance of wall constructions due to the influence of linear and point thermal bridges. Theodosiou et al. (2017) investigated the nature of thermal bridge effects in ventilated facades, proving that proper design can significantly contribute to an optimum result [21]. Theodosiou (2008) presented a study on representative wall thermal insulation configurations used in Greek buildings, in order to investigate the impact of the thermal bridges on the energy consumption [22]. Zalewski et al. (2010) performed the quantitative evaluation of heat losses through industrial light structure walls made of metal framework, where insulation material was installed in between metal trusses, with the water vapor barrier and the internal and external coatings. This study showed that the heat losses in place of steel frame were more than twice as intensive as elsewhere [1]. Different methods are used to evaluate the influence of thermal bridges on the heat transfer: numerical calculation, standard formulas, measurements. Larbi (2004) presented regression models of the thermal transmittance for three linear thermal bridges: slab-on-grade floor-wall junction, floor-wall junction, and roof-wall junction. For all models, the relative errors were less than 5%, which summed with errors obtained from numerical calculations (about 5%) would be around 10%, which were less than the errors generally obtained using calculation formulas [20].

It is essential to minimize the heat losses of energy efficient buildings in the design and building phases, especially in a cold climate, where a large part of the space heating demand is caused by transmission losses through the building envelope [23]. Thermal bridges play a major role in the thermal losses of the building envelope and should be minimized, especially under winter dominant conditions and for high cooling degree day regions in Europe and worldwide [24]. In the case of new buildings, an explicit calculation of thermal bridges is used in 35% of the countries in North Europe, 100% in Central Europe, and 50% in South Europe [25].

Typically, when calculating the heat transfer coefficient of a partition and modelling linear (and point) thermal bridges, the joints passing through the thermal insulation are evaluated [1,26]; however, the influence of facings is not evaluated. In some cases, it is recommended to remove the facings from the materials in the area of connection, to bond the products by gluing at the corners, but in practice, polyisocyanurate foam products are often bonded without removing the facings. Therefore, this study is conducted to evaluate the extent to which a facing can influence heat transfer through partitions, especially when the facing is made of aluminum foil tin.

Studies investigating the effect of PIR thermal insulation facings on heat loss have not been found, but very similar studies have been performed with vacuum insulation panels (VIP). These studies also analyzed the influence of very thin and high thermal conductivity facings (usually, aluminum foil) on the heat loss and the formation of linear thermal bridges around the joints between the two connected plates [27,28].

This article is structured as follows: Section 2 covers the description of the materials and methods used in the numerical calculation and experimental measurements of this study. The results of the numerical calculation and its verification by experimental measurement are presented in Section 3. The discussion is given in Section 4.

## 2. Methods and Measuring Equipment

### 2.1. Structure and Materials of Wall Fragments for Investigation

The structure of the ventilated wall modelled for numerical calculation is shown in Figure 2.

**Table 1.** Wall materials.

No.	Material	Thickness, mm	Thermal Conductivity $\lambda$ , W/(m·K)
1	Plaster	10	0.9
2	Aerated concrete blocks	200	0.13
3	PU foam	$\leq 10$	0.04
4	PIR boards with facing:	100	0.022
	(a) aluminum foil	100 $\mu\text{m}$	211
	(b) multilayer aluminized facing	155 $\mu\text{m}$	0.125
	(c) composite paper facing	132 $\mu\text{m}$	0.066
	(d) plastic facing	103 $\mu\text{m}$	0.125

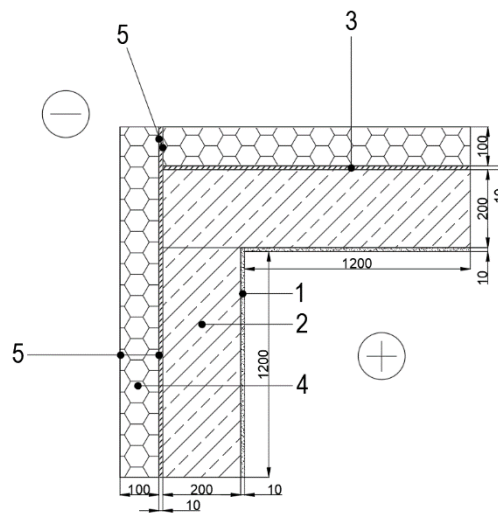


**Figure 2.** Fragment of the wall corner: 1—plaster, 2—aerated concrete blocks, 3—PU foam, 4—PIR insulation, 5—PIR facings (see Table 1) (all the dimensions are expressed in millimeters).

The thermal transmittance value ( $U$ -value) of the wall was selected in accordance with the recommendations of European Insulation Manufacturers Association (EURIMA) [29] and the Nearly Zero Energy Buildings (NZEB) requirements for buildings constructed in a northern climate [30]. The  $U$ -value of  $0.15 \text{ W}/(\text{m}^2 \cdot \text{K})$  falls within the range of  $U$ -values of walls in EU countries of the Nordic region, where they vary between  $0.12 \text{ W}/(\text{m}^2 \cdot \text{K})$  and  $0.17 \text{ W}/(\text{m}^2 \cdot \text{K})$  [3]. The  $U$ -value of walls ( $U = 0.15 \text{ W}/(\text{m}^2 \cdot \text{K})$ ) for this study was calculated in accordance with EN ISO 6946:2017 [31].

The structure consisted of 10 mm internal plaster, a 200 mm aerated concrete block masonry, a 10 mm thick PU glue layer, and a 100 mm PIR insulation layer (thermal properties are given in Table 1), as well as a ventilated air gap and exterior cladding (not shown in Figure 2). Different diffusion-proof facings of PIR insulation were chosen, so that the declared thermal conductivity could be retained.

PIR thermal insulation with four different facings was used in these wall fragments: multilayer aluminized facing, aluminum foil, composite paper facing, and plastic facing, as well as unfaced PIR and PU glue at the joint of PIR boards.

The influence of studs and fasteners was not evaluated for the modelled wall fragment, because this is a comparative study, so the results do not depend much on the evaluation of studs and fasteners, as the influence of these elements would be the same in all cases studied. The results obtained cannot be directly applied to the determination of the heat transfer coefficients of linear thermal bridges at similar wall corners, as there will be different fasteners, with different dimensions and quantities in each case.

The specimens for experimental measurement were made from two 100 mm thick PIR boards with aluminum foil tin facing and multilayer aluminized facing. For initial R-value measurement, PIR boards (dimensions  $600 \times 600 \text{ mm}$ ) with facings as produced were used, and after that, a strip  $100 \times 100 \text{ mm}$  in width (equal to thickness of specimen) with facings was cut from the center of the specimen

and rotated 90 degrees to expose the facings to the middle of the specimen (Figure 3). Thus, in the new specimen, a facing appeared in the direction of the heat flow, forming a linear thermal bridge.

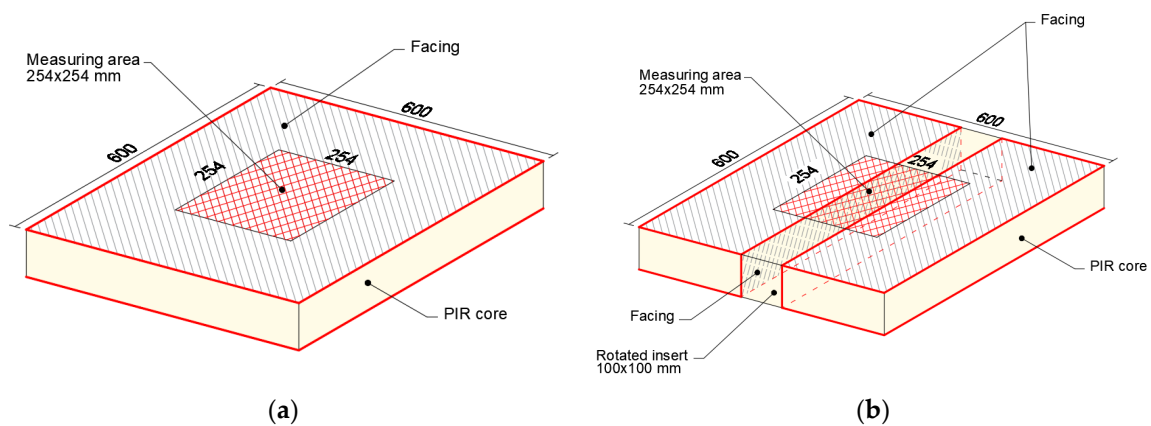


**Figure 3.** Specimens with a marked measuring area: (a) continuous specimen, (b) specimen with rotated insert (all the dimensions are expressed in millimeters).

## 2.2. Numerical Calculation of Heat Transfer through Building Corner Joints Insulated with Faced Polyurethane Products

The computer software THERM 7 developed at Lawrence Berkeley National Laboratory (LBNL), which complies with the standard EN ISO 10211:2017, was used for modelling of heat transfer through the building corner joints. THERM 7 is two-dimensional heat-transfer calculation tool for building components such as windows, walls, foundation, roofs, and doors where changes of thermal uniformity are of concern [32]. The 2D model was chosen for the investigation, because the linear thermal bridge was formed in the corner of the wall [20]. THERM's heat-transfer analysis is based on the finite-element method, dedicated to model composite structures of complicated geometry and of different thermal conductivity building materials. The  $\Psi$ -value represents the difference of heat flow through the 2D element when calculating using the finite-element method (assumed as real) and the sum of heat flow through the 1D elements constituting the composite structure, in our case the wall corner. The thermal transmittance coefficient of linear thermal bridge  $\Psi$  can be defined as the added heat flux through a thermal bridge with respect to the same solution without the thermal bridge per meter of length when a temperature difference of 1 °C is applied between both sides [33]. The difference in thermal transmission coefficients of the thermally interrupted 2D element and the uninterrupted 2D element represents the impact of interruptions on heat flow passing the corner. The temperature distribution and the heat flux intensity charts are used for visual demonstration of this impact.

According to the standard EN ISO 10211:2017 [34], the linear thermal transmittance considered of the linear thermal bridge separating two environments,  $\Psi$ , is given by:

$$\Psi = L_{2D} - \sum_{j=1}^{N_j} U_j \cdot l_j, \text{ W}/(\text{m}\cdot\text{K}) \quad (1)$$

where:  $L_{2D}$ —the thermal coupling coefficient obtained from a 2D calculation of the component separating the two environments being considered,  $\text{W}/(\text{m}\cdot\text{K})$ ;  $U_j$ —the thermal transmittance of the 1D component  $j$  separating the two environments being considered,  $\text{W}/(\text{m}^2\cdot\text{K})$ ;  $l_j$ —the length within the 2D geometrical model over which the value  $U_j$  applies, based on outdoor length, m;  $N_j$ —the number of 1D components.

For this numerical calculation, boundary temperatures  $\theta_{int} = 20$  °C and  $\theta_e = 0$  °C and the heat transfer resistances of the surfaces  $R_{si} = 0.13$  ( $\text{m}^2\cdot\text{K})/\text{W}$  and  $R_{se} = 0.04$  ( $\text{m}^2\cdot\text{K})/\text{W}$  were selected.

The heat transfer coefficient of the linear thermal bridge of modelled building corners insulated with faced PIR boards was compared to the heat transfer coefficient of the linear thermal bridge of the same corner insulated with a single layer of PIR without facing, and PU glue in the joint. The difference

in the result values obtained was the only indicator of the impact of different facings and PU glue on the heat transfer through the insulated wall corner of the building. The increment of the heat flow rate through the 1 m of corner due to the impact of facings  $\Delta\Phi$  was calculated using equation:

$$\Delta\Phi = (L_{2D}^F - L_{2D}^R) \cdot \Delta\theta, \text{ W/m} \quad (2)$$

where:  $L_{2D}^F$ —the thermal coupling coefficient, calculated for a wall corner insulated with faced PIR insulation,  $\text{W}/(\text{m}\cdot\text{K})$ ;  $L_{2D}^R$ —the thermal coupling coefficient, calculated for a wall corner insulated with PIR insulation without facings,  $\text{W}/(\text{m}\cdot\text{K})$ ;  $\Delta\theta$ —the difference of internal and external temperatures used for the calculation of heat losses,  $\text{K}$ .

### 2.3. Experimental Measurement of the Influence of a Facing on the Heat Transfer through a Thermal Insulating Material with a Facing

The evaluation of thermal bridges can be done experimentally by using standardized measurement methods on two building elements of the same design, the first one with and the second one without a thermal bridge [20]. The heat transfer through the building element (thermal resistance) can be measured using a heat flow meter apparatus; in our case, it was Fox 600 (developed by TA Instruments, USA). The heat flow meter apparatus was made of two plates, where heat flow meters were installed, which were placed above and below the specimen. The dimensions of heat flow meter's plates were  $600 \times 600$  mm, and measurement area of the heat flow meter was  $254 \times 254$  mm. Set point temperatures were kept constant during all the tests:  $\theta_i = 20$  °C and  $\theta_e = 0$  °C. No internal and external surface resistances were considered.

The principle of measurement was to create a constant temperature difference between the bottom and top plates and to measure the specific heat flow and surface temperatures under constant temperature conditions.

The  $R$ -value of the measured specimen was calculated according to the following equation:

$$R = \frac{\Delta\theta}{q}, (\text{m}^2\cdot\text{K})/\text{W} \quad (3)$$

where:  $\Delta\theta$  is the temperature difference on opposite surfaces of the measured specimen,  $\text{K}$ ;  $q$  is the heat flow rate passing through the specimen,  $\text{W}/\text{m}^2$ ; the thermal conductivity of material  $\lambda$ ,  $\text{W}/(\text{m}\cdot\text{K})$  is calculated according to this equation:

$$\lambda = \frac{d}{R}, \text{ W}/(\text{m}\cdot\text{K}) \quad (4)$$

where:  $d$ —thickness of the specimen,  $\text{m}$ .

Although the heat flow meter apparatus was designated to determine the thermal resistance and thermal conductivity of a solid material, according to Lorenzati et al. (2004), the equivalent thermal resistance  $R_e$  of composite specimens made from different thermal conductivity materials could be determined [35]. In this case, the difference of the average surface temperatures of the test specimen was used to calculate the  $R_e$ -value. Equivalent thermal conductivity coefficient of the specimen with thermal interruption  $\lambda_e$  was calculated from  $R_e$  using Equation (4).

The heat transfer coefficient of the linear thermal bridge formed in the test sample is given by the equation:

$$\varphi = \frac{(U_e - U) \cdot A}{2l} = \frac{A \cdot \left( \frac{\lambda_e}{d} - \frac{\lambda}{d} \right)}{2l} = \frac{A \cdot (\lambda_e - \lambda)}{2l} = \frac{A}{d \cdot 2l} \cdot (\lambda_e - \lambda), \text{ W}/(\text{m}\cdot\text{K}) \quad (5)$$

where:  $l$ —the length of the linear thermal bridge, formed in the specimen, equal to the length of the measurement area of the heat flow meter, 0.254 m;  $A$ —measurement area,  $\text{m}^2$ ;  $\lambda$ —thermal conductivity

of the continuous specimen,  $W/(m \cdot K)$ ;  $\lambda_e$ —equivalent thermal conductivity of the specimen with facing inside,  $W/(m \cdot K)$ .

The increment of the heat flow rate through the 1 m connection of the PIR boards with facings  $\Delta\Phi$ ,  $W/m$ , was calculated using equation:

$$\Delta\Phi = \varphi \cdot \Delta\theta, \text{ W/m} \quad (6)$$

### 3. Results

#### 3.1. Results of the Numerical Calculation

Figure 4 shows the heat flow rate through the corners insulated with PIR faced with different facings. Using Equation (2), the calculated difference of heat flow between the corner of the wall insulated with PIR with aluminum foil facing and insulated with PIR without facing was  $\Delta\Phi = 0.484 \text{ W/m}$ , and for specimens with other facings  $\Delta\Phi = 0.001 \text{ W/m}$ . These numbers proved that aluminum foil raised the heat flow through the construction compared to other facing materials and should be evaluated.

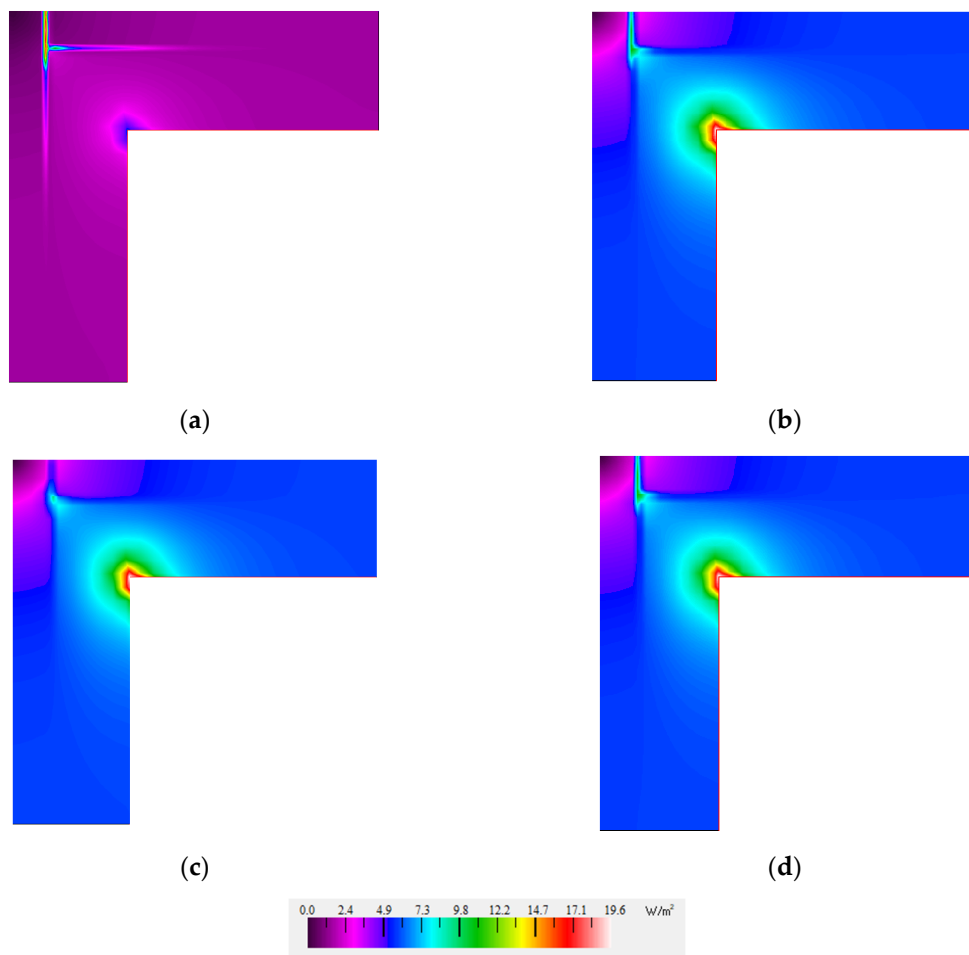


**Figure 4.** The heat flow rate through the corners of the wall insulated with PIR, faced with different facings: (a) aluminum foil, (b) multilayer aluminized facing, (c) composite paper facing, (d) plastic facing.

The results obtained (Table 2) showed that the value of the thermal bridge when multilayer aluminized facing, composite paper facing, or plastic facing were used was equal. This was because these facings had a very similar thermal conductivity, which was close to the thermal conductivity of the PIR thermal insulating material, and therefore, their influence on the value of the thermal bridge

was very small. As in the case with aluminum foil, even a very thin facing could make the situation worse. When using PIR insulation without facings, the calculated  $U$ -value was close to the case when PIR was used with facings, which had a similar thermal conductivity as PIR itself.

**Table 2.** Calculation results.

Construction Type	$L_{2D}$	Thermal Bridge Value, $\Psi$ , W/(m·K)	$\Delta\Phi$ , W/m	
Wall corner insulated with PIR with different types of facings and with PU glue in the joint between two boards in the corner (Figure 4)	(a) aluminum foil	0.2834	−0.017	
	(b) multilayer aluminized facing	0.2592		
	(c) composite paper facing	0.2590	−0.041	0.001 0.484
	(d) plastic facing	0.2592		
Wall corner insulated with PIR without any facing and with PU glue in the joint between two boards in the corner (Figure 5)	0.2592	−0.041		
Wall corner insulated with PIR with aluminum foil facing, without facing and with PU glue in the joint between two boards in the corner (Figure 6)	0.2636	−0.036	0.088	
Wall corner insulated with PIR with aluminum foil facing, with facing and without PU glue in the joint between two boards in the corner (Figure 7a)	0.2948	−0.005	0.72	
Wall corner insulated with PIR without any facing and without PU glue in the joint between two boards in the corner (Figure 7b)	0.2588	−0.041		
Wall corner insulated with PIR with aluminum foil facing, with removed facing and PU glue in the joint between two boards in the corner (Figure 8)	0.2628	−0.037	0.08	

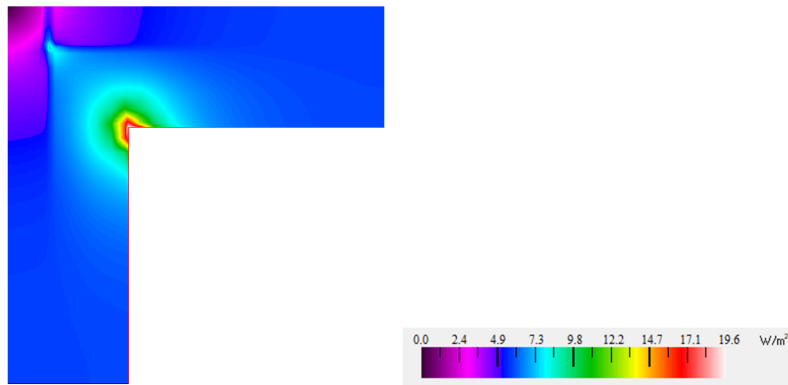


**Figure 5.** The heat flow rate through the wall corner insulated with PIR without facing.

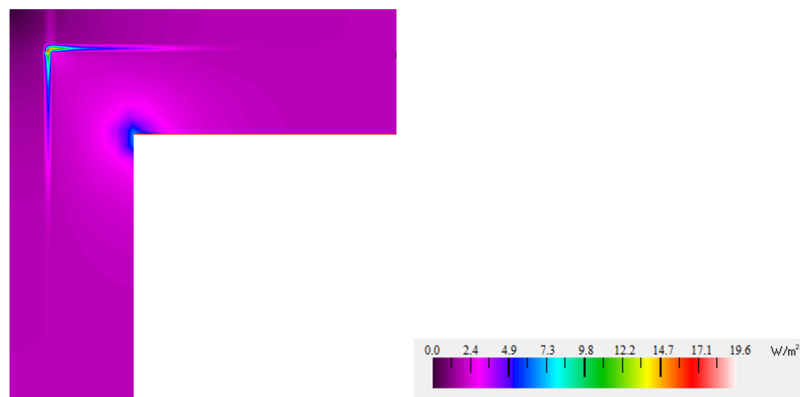


**Figure 6.** The heat flow rate through the wall corner insulated with aluminum foil-faced PIR, without aluminum foil at the joint between boards and with PU glue in the joint.

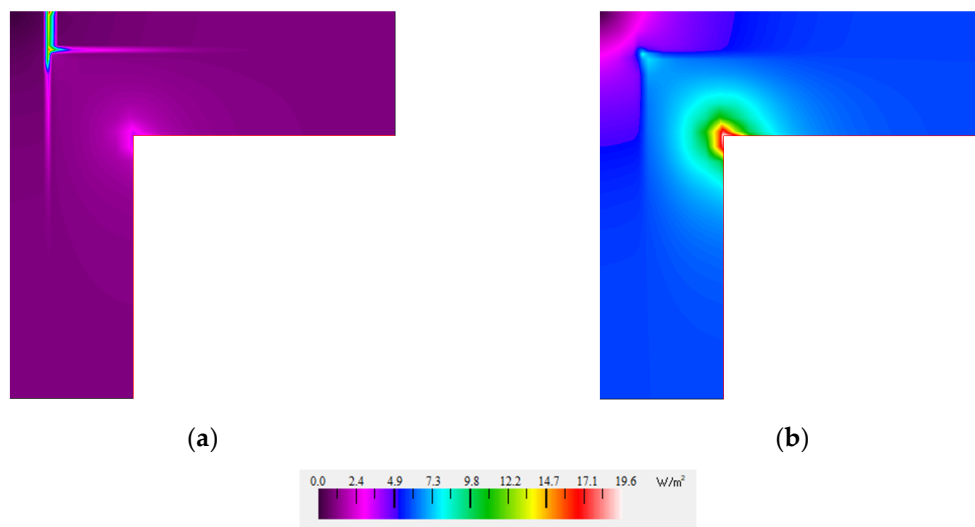


**Figure 7.** The heat flow rate through the wall corner insulated with: (a) aluminum foil-faced PIR, without PU glue in the joint; (b) PIR without facing and without PU glue in the joint.

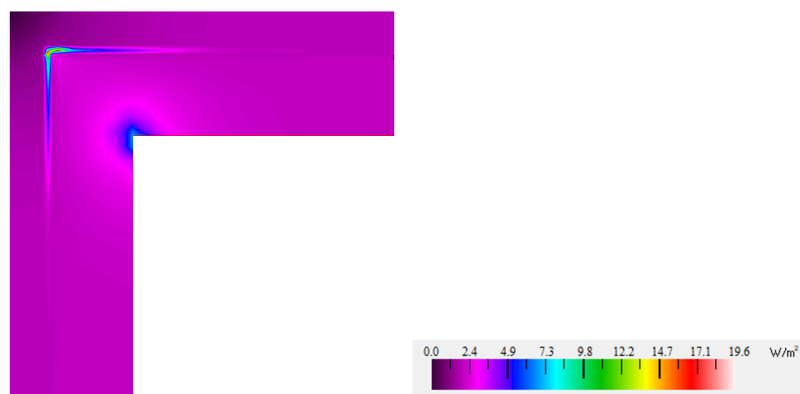


**Figure 8.** The heat flow rate through the wall corner insulated with aluminum foil-faced PIR, with removed aluminum foil and without PU glue in the joint.

In the modelled wall corners, a 10 mm PU glue layer was used in the PIR insulation joint so that the aluminum foil facing on the joint did not come into contact to the aluminum foil facing on the outside surface of the connecting PIR board.

Given that the results of PIR with aluminum facing were different from other options and the corners with the rest of the facings had identical values, it was decided to analyze the corner, insulated with PIR board without facings. Figure 5 shows the intensity of heat flow through the corner insulated with PIR without any facings, but with PU glue in the joint between two boards.

It was observed that the corners with PIR insulation without facings and with PIR insulation with other than aluminum facings had the same values, so it was decided not to evaluate PIR facing if it was not aluminum. It could be said that PIR faced with composite paper, multilayer aluminized facing, or plastic facing gave the same results as PIR without facings. All later comparisons in this study were made between PIR with aluminum facing and PIR without facings.

Another modelled corner construction was PIR with removed aluminum foil facing at the joint between boards, using PU glue in this gap. The heat flow rate of this construction is given in Figure 6. It can be compared to the construction given in Figure 5, as this construction had PIR without any facing and PU glue in the joint. The difference of the heat flow between these two constructions was  $\Delta\Phi = 0.088$  W/m and could be evaluated as having little significance.

Since PU glue is not commonly used in the joint, we considered the situation where the aluminum foil facing in the joint is in contact with both PIR insulation aluminum foil facings on the outside and at the inside surfaces of adjacent PIR board. For comparison, another simulation for PIR without facing and without PU glue was performed. The simulation results are presented in Figure 7.

The linear thermal bridge was calculated, and its value was  $\Psi = -0.005$  W/(m·K) for the wall corner insulated with aluminum foil-faced PIR (Figure 7a) and  $\Psi = -0.041$  W/(m·K) for the wall corner insulated with PIR without facing (Figure 7b). As can be noticed, when calculating the thermal bridge of the wall corner insulated with PIR with other than aluminum foil facings, PU glue in the corner joint between two boards could not be evaluated. The difference of heat flow between these two variants was  $\Delta\Phi = 0.72$  W/m, and this meant that not using PU glue in the joint, the heat flow through the wall corner constructions rose.

In order to reduce the heat flow to the outside, which was increasing through the aluminum foil facing at the joint of the PIR insulation boards, it was necessary to remove the facing at this joint (Figure 8). In this case, the linear thermal transmittance value was  $\Psi = -0.037$  W/(m·K). Then, the difference of heat flow between PIR insulation with aluminum foil facing, removed aluminum foil, and PU glue in the joint and PIR insulation without facing and without PU glue in the joint (Figure 7b) was calculated using Equation (2), which was  $\Delta\Phi = 0.08$  W/m, or 8.5 times lower than the constructions shown in Figure 6.

All results of the numerical simulations are summarized in Table 2.

### 3.2. Results of Experimental Measurement of Heat Transfer through the Specimens with Thermal Interruptions

The results of experimental measurement of continuous PIR boards with aluminum foil tin facing and multilayer aluminized facing and the same boards with a rotated insert, when part of facings was positioned parallel to the heat flow and created the thermal bridge, are summarized in Table 3.

**Table 3.** Results of the experimental measurements.

Facing Type	Specimen Type	$R$ , (m <sup>2</sup> ·K)/W	$d$ , m	$\lambda$ , W/(m·K)	$A$ , m <sup>2</sup>	$l$ , m	$\varphi$ , W/(m·K)	$\Delta\Phi$ , W/m
Aluminum foil facing	Continuous specimen	3.69	0.101	0.027	0.064	0.254	0.035	0.70
	Specimen with rotated insert	1.83		0.055				
Multilayer aluminized facing	Continuous specimen	3.50	0.102	0.029	0.064	0.254	0.019	0.38
	Specimen with rotated insert	2.32		0.044				

It can be noticed in Table 3 that the thermal resistances were quite similar in both PIR samples with aluminum foil and multilayer aluminized facing. The heat resistance of the sample with aluminum facing was slightly higher because aluminum is a more heat conductive material; therefore, more intense heat propagation perpendicular to the heat flow occurred, resulting in lateral heat loss and decreasing measurement accuracy. However, this measurement was comparative; the difference in thermal resistance obtained did not significantly influence the result of the experiment.

The measured equivalent thermal resistances of the samples with rotated inserts, i.e., with formed thermal bridges from different facings, differed from each other and from the continuous samples. The measured thermal resistance of aluminum-faced specimens was approximately two times bigger than the equivalent thermal resistance of the same specimens with a formed thermal bridge, and the difference between these thermal resistances of multilayer aluminized facing was approximately 33%.

The equivalent thermal resistance of the specimen with a thermal bridge formed of the aluminum foil was approximately 20% lower than those specimens with inserts made of multilayer aluminized facing. Comparing the heat transfer values of the thermal bridges of both specimens, it can be noticed that in the case of aluminum facing, this value almost doubled.

#### 4. Discussion and Conclusions

The results of the numerical simulations and experimental measurements confirmed that significant heat losses occurred at the wall corners insulated with PIR thermal insulation with aluminum facing and should be considered when calculating the thermal transmittance of the linear thermal bridge of such a construction. The numerical simulation results showed that the heat flow through the joint of the walls with a  $U$ -value of  $0.15 \text{ W}/(\text{m}^2 \cdot \text{K})$  (1 m per each wall) was  $0.484 \text{ W}$  per 1 m of wall height. For a medium-sized single-family dwelling, this amounted to  $3\text{--}4 \text{ kWh}/\text{m}^2$  per year. The experimental measurement also clearly showed that the aluminum foil insert reduced the thermal resistance of the 100 mm thick PIR thermal insulation board twice, although the insertion area represented only about 0.1% of the sample measuring area.

Numerical simulations of wall corner joints insulated with PIR thermal insulation boards with other than aluminum foil facings showed that their influence on the heat transfer through the wall joints could not be evaluated. The heat flow through the connection of the tested wall with these facings did not exceed  $0.001 \text{ W}$  and, therefore, could not have a significant effect on the heat loss of the building.

Analyzing heat transfer through modelled wall corners insulated with PIR thermal insulation boards with aluminum facing, differences in the heat transfer depending on the contact between two boards creating a corner were observed. The numerical simulation was performed for the wall corner insulated with PIR boards with aluminum foil facing in two cases: when PU glue was used in the contact joint between thermal insulation boards (Figure 4a) and without PU glue in the joint (Figure 7a). In the second case, the external and internal aluminum facings of one of the connecting boards were joined by the aluminum facing of the contacting surface of the other board. The thermal coupling coefficient value  $L_{2D}$  for the construction with PU glue was  $0.2834 \text{ W}/(\text{m} \cdot \text{K})$  and for the construction without PU glue was  $0.2948 \text{ W}/(\text{m} \cdot \text{K})$ . This meant that the effect of breaking the contact using a glue layer between the facings of the PIR thermal insulation boards on the heat flux through the joint was about  $0.23 \text{ W}$  per 1 m of wall joint height. The top and bottom facings of the specimen were joined by the facings of rotated heat-conductive inserts, and the specimens were measured in a heat flow meter apparatus. Unexpectedly, a 33% reduction in thermal resistance was observed when comparing continuous specimens and specimens with rotated inserts with a multilayer aluminized facing, although numerical simulation showed the minimal influence of this facing on the heat transfer through the corner of the wall. This may be due to the contact of the rotated insert facing with the top and bottom measuring plates of the heat flow meter apparatus, possibly altering the cell data of the heat flow meter. Summarizing the results of the numerical modelling and experimental measurement, it can be stated that the PU glue layer used for joining two PIR thermal insulation

boards with aluminum facing worked in two ways: the heat transfer through the joint was increased, because the thermal conductivity of PU glue was higher than of the PIR core, and on the other hand, the PU prevented the facing of one thermal insulation board from joining the inner and outer facings of another thermal insulation board, thus reducing overall heat transfer through the wall corner joint. Therefore, it was possible to determine the importance of not forming a joint in the direction of the heat flux between the aluminum facings of the internal and external PIR thermal insulation boards only based on experimental measurement results.

The study was not extensive and detailed enough to define the conditions for installing PIR thermal insulation boards with aluminum facing in a wall corner. The influence of PIR thermal insulation boards with aluminum facings was found to be significant; however, it remains unclear how the heat transfer through the corner of PIR thermal insulation boards with removed facing will change over the time of operation, when, after removal of the facing, the thermal conductivity of the PIR core will increase due to the gas diffusion. Therefore, further research to find answers to these questions is planned.

**Author Contributions:** The three authors contributed to this paper as follows: conceptualization, T.M. and R.B.; methodology, T.M., R.B., and A.B.; formal analysis, T.M. and R.B.; investigation, T.M. and A.B.; resources, T.M.; data curation, T.M. and A.B.; writing, original draft preparation, T.M.; writing, review and editing, R.B.; visualization, T.M.; supervision, R.B.; project administration, R.B. All authors read and agreed to the published version of the manuscript.

**Funding:** This research received no external funding.

**Conflicts of Interest:** The authors declare no conflict of interest.

## References

1. Zalewski, L.; Lassue, S.; Rousse, D.; Boukhalfa, K. Experimental and numerical characterization of thermal bridges in prefabricated building walls. *Energy Convers. Manag.* **2010**, *51*, 2869–2877. [[CrossRef](#)]
2. Pérez-Bella, J.; Domínguez-Hernández, J.; Cano-Suñén, E.; Alonso-Martínez, M.; del Coz-Díaz, J.J. Details territorial estimation of design thermal conductivity for façade materials in North-Eastern Spain. *Energy Build.* **2015**, *102*, 266–276. [[CrossRef](#)]
3. Paraschiv, L.S.; Paraschiv, S.; Ion, I.V. Increasing the energy efficiency of buildings by thermal insulation. In Proceedings of the International Scientific Conference “Environmental and Climate Technologies”, Riga, Latvia, 10–12 May 2017. [[CrossRef](#)]
4. Sadineni, S.B.; Madala, S.; Boehm, R.F. Passive building energy savings: A review of building envelope components. *Renew. Sustain. Energy Rev.* **2011**, *15*, 3617–3631. [[CrossRef](#)]
5. Berardi, U. The impact of temperature dependency of the building insulation thermal conductivity in the Canadian climate. In Proceedings of the 11th Nordic Symposium on Building Physics, Trondheim, Norway, 11–14 June 2017. [[CrossRef](#)]
6. Zhang, H.; Fang, W.; Li, Y.; Tao, W. Experimental study of the thermal conductivity of polyurethane foams. *Appl. Therm. Eng.* **2017**, *115*, 528–538. [[CrossRef](#)]
7. Jin, J.; Dong, Q.; Shu, Z.; Wang, W.; He, K. Flame retardant properties of polyurethane/expandable graphite composites. *Procedia Eng.* **2014**, *71*, 304–309. [[CrossRef](#)]
8. Biswas, K.; Desjarlais, A.; Smith, D.; Letts, J.; Yao, J.; Jiang, T. Development and thermal performance verification of composite insulation boards containing foam-encapsulated vacuum insulation panels. *Appl. Energy* **2018**, *228*, 1159–1172. [[CrossRef](#)]
9. Walker, R.; Pavía, S. Thermal performance of a selection of insulation materials suitable for historic buildings. *Build. Environ.* **2015**, *94*, 155–165. [[CrossRef](#)]
10. Bynum, R.T., Jr. *Insulation Handbook*; McGraw-Hill: New York, NY, USA, 2000; pp. 205–241.
11. Al-Homoud, M.S. Performance characteristics and practical applications of common building thermal insulation materials. *Build. Environ.* **2005**, *40*, 353–366. [[CrossRef](#)]
12. Feldman, D. Polymeric foam materials for insulation in buildings. In *Materials for Energy Efficiency and Thermal Comfort in Buildings*; Hall, M.R., Ed.; Woodhead Publishing: Cambridge, UK, 2010; pp. 257–273.

13. PU Europe Technical Report on Thermal Insulation Materials Made of Rigid Polyurethane Foam (PUR/PIR). Available online: <https://www.pu-europe.eu/library/pu-europe-reports/> (accessed on 15 February 2020).
14. Types of Laminated PIR Boards. Available online: <http://www.poliuretanos.com/en/productos/laminados/pur-al.html> (accessed on 14 April 2020).
15. Technical Bulletin 117: A Guide to the Classification of Polyiso Board Insulation Products. Available online: <https://www.polyiso.org/page/100SeriesRoofing> (accessed on 15 February 2020).
16. Mukhopadhyaya, P.; Bomberg, M.T.; Kumaran, M.K.; Drouin, M.; Lackey, J.; van Reenen, D.; Normandin, N. Long-term thermal resistance of polyisocyanurate foam insulation with impermeable facers. In *Insulation Materials: Testing and Applications*; Desjarlais, A.O., Zarr, R.R., Eds.; ASTM International: West Conshohocken, PA, USA, 2002; Volume 4, pp. 351–365.
17. Stovall, T. *Closed Cell Foam Insulation: A Review of Long Term Thermal Performance Research*; Oak Ridge National Laboratory: Oak Ridge, TN, USA, 2012.
18. Bogdan, M.; Hoerter, J.; Moore, F.O. Meeting the insulation requirements of the building envelope with polyurethane and polyisocyanurate foam. *J. Cell. Plast.* **2005**, *41*, 41–56. [[CrossRef](#)]
19. Marrucho, I.M.; Santos, F.; Oliveira, N.S.; Dohrn, R. Aging of rigid polyurethane foams: Thermal conductivity of N<sub>2</sub> and cyclopentane gas mixtures. *J. Cell. Plast.* **2005**, *41*, 207–224. [[CrossRef](#)]
20. Larbi, A.B. Statistical modelling of heat transfer for thermal bridges of buildings. *Energy Build.* **2005**, *37*, 945–951. [[CrossRef](#)]
21. Theodosiou, T.; Tsikaloudaki, K.; Bikas, D. Analysis of the thermal bridge effect on ventilated facades. In Proceedings of the International Conference on Sustainable Synergies from Buildings to the Urban Scale, Thessaloniki, Greece, 16–19 October 2016. [[CrossRef](#)]
22. Theodosiou, T.G.; Papadopoulos, A.M. The impact of thermal bridges on the energy demand of buildings with double brick wall constructions. *Energy Build.* **2008**, *40*, 2083–2089. [[CrossRef](#)]
23. Berggren, B.; Wall, M. Calculation of thermal bridges in (Nordic) building envelopes—Risk of performance failure due to inconsistent use of methodology. *Energy Build.* **2013**, *65*, 331–339. [[CrossRef](#)]
24. Cerneckiene, J.; Zdankus, T.; Valancius, R.; Fokaides, P.A. Numerical investigation of the impact of longitudinal thermal bridging on energy efficient buildings under humid continental climate conditions: The case of Lithuania. *IOP Conf. Ser. Earth Environ. Sci.* **2020**, *410*, 105. [[CrossRef](#)]
25. Impact of Thermal Bridges on the Energy Performance of Buildings. Available online: <https://www.buildup.eu/en/practices/publications/impact-thermal-bridges-energy-performance-buildings> (accessed on 9 March 2020).
26. Levinskytė, A.; Bliūdžius, R.; Burlingis, A.; Makaveckas, T. Dependencies of heat transmittance through the ventilated wall system on thermal conductivity of connectors crossing thermal insulation layer. In Proceedings of the 4th Central European Symposium on Building Physics, Prague, Czech Republic, 2–5 September 2019; EDP Sciences: Les Ulis, France, 2019. [[CrossRef](#)]
27. Tenpierik, M.; Cauberg, H. Analytical Models for Calculating Thermal Bridge Effects Caused by Thin High Barrier Envelopes around Vacuum Insulation Panels. *J. Build. Phys.* **2007**, *30*, 185–215. [[CrossRef](#)]
28. Schwab, H.; Stark, C.; Wachtel, J.; Ebert, H.P.; Fricke, J. Thermal Bridges in Vacuum-insulated Building Façades. *J. Therm. Envel. Build. Sci.* **2005**, *28*, 345–355. [[CrossRef](#)]
29. U-Values in Europe. Available online: <https://www.eurima.org/u-values-in-europe/> (accessed on 15 February 2020).
30. Ahmed, K.; Carlier, M.; Feldmann, C.; Kurnitski, J. A new method for contrasting energy performance and near-zero energy building requirements in different climates and countries. *Energies* **2017**, *10*, 334. [[CrossRef](#)]
31. EN ISO 6946. *Building Components and Building Elements—Thermal Resistance and Thermal Transmittance—Calculation Methods 2017*; ISO: Geneva, Switzerland, 2017.
32. Two-Dimensional Building Heat-Transfer Modeling. Available online: <https://windows.lbl.gov/software/therm> (accessed on 9 March 2020).
33. Martin, K.; Campos-Celador, A.; Escudero, C.; Gómez, I.; Sala, J.M. Analysis of a thermal bridge in a guarded hot box testing facility. *Energy Build.* **2012**, *50*, 139–149. [[CrossRef](#)]

34. EN ISO 10211. *Thermal Bridges in Building Construction—Heat Flows and Surface Temperatures—Detailed Calculations 2017*; ISO: Geneva, Switzerland, 2017.
35. Lorenzati, A.; Fantucci, S.; Capozzoli, A.; Perino, M. The effect of different materials joint in Vacuum Insulation Panels. In Proceedings of the 6th International Conference on Sustainability in Energy and Buildings, Cardif, Wales, UK, 25–27 June 2014. [[CrossRef](#)]



© 2020 by the authors. Licensee MDPI, Basel, Switzerland. This article is an open access article distributed under the terms and conditions of the Creative Commons Attribution (CC BY) license (<http://creativecommons.org/licenses/by/4.0/>).